Biochimica et Biophysica Acta 1853 (2015) 2104–2114

Contents lists available at ScienceDirect

Biochimica et Biophysica Acta

journal homepage: www.elsevier.com/locate/bbamcr

The transmembrane Bax inhibitor motif (TMBIM) containing protein family: Tissue expression, intracellular localization and effects on the ER CA^{2+}-filling state☆

Dmitrij A. Lisak [a], Teresa Schacht [a], Vitalij Enders [a], Jörn Habicht [a], Santeri Kiviluoto [b], Julia Schneider [a], Nadine Henke [a], Geert Bultynck [b], Axel Methner [a,*]

[a] Focus Program Translational Neuroscience (FTN), Rhine Main Neuroscience Network (rmn²), Department of Neurology, Johannes Gutenberg University Medical Center Mainz, Langenbeckstr. 1, Mainz D-55131, Germany

[b] Laboratory of Molecular and Cellular Signaling, Department of Cellular and Molecular Medicine, KU Leuven, Campus Gasthuisberg O/N-I bus 802, Herestraat 49, Leuven BE-3000, Belgium

ARTICLE INFO

Article history:
Received 18 September 2014
Received in revised form 19 January 2015
Accepted 1 March 2015
Available online 9 March 2015

Keywords:
RECS1
FAIM2
GRINA
GAAP
GHITM
MICS1

ABSTRACT

Bax inhibitor-1 (BI-1) is an evolutionarily conserved pH-dependent Ca^{2+} leak channel in the endoplasmic reticulum and the founding member of a family of six highly hydrophobic mammalian proteins named transmembrane BAX inhibitor motif containing (TMBIM) 1-6 with BI-1 being TMBIM6. Here we compared the structure, subcellular localization, tissue expression and the effect on the cellular Ca^{2+} homeostasis of all family members side by side. We found that all TMBIM proteins possess the di-aspartyl pH sensor responsible for pH sensing identified in TMBIM6 and its bacterial homologue BsYetJ. TMBIM1-3 and TMBIM4-6 represent two phylogenetically distinct groups that are localized in the Golgi apparatus (TMBIM1-3), endoplasmic reticulum (TMBIM4-6) or mitochondria (TMBIM5) but share a common structure of at least seven transmembrane domains with the last domain being semi-hydrophobic. TMBIM1 is mainly expressed in muscle, TMBIM2 and 3 in the nervous system, TMBIM4 and 5 are ubiquitously expressed and TMBIM6 in skeletal muscle, kidney, liver and spleen. All TMBIM proteins reduce the Ca^{2+} content of the endoplasmic reticulum, and all but TMBIM5 also reduce the cytosolic resting Ca^{2+} concentration. These results suggest that the TMBIM family has comparable functions in the maintenance of intracellular Ca^{2+} homeostasis in a wide variety of tissues. This article is part of a Special Issue entitled: 13th European Symposium on Calcium. Guest Editors: Jacques Haiech, Claus Heizmann and Joachim Krebs.

1. Introduction

BAX inhibitor-1 (BI-1) is an anti-apoptotic protein of seven transmembrane domains first identified in a screen for human proteins capable of inhibiting BAX-mediated cell death in yeast [1]. In mammals, its cytoprotective properties are most evident in paradigms of endoplasmic reticulum (ER) stress and ischemia/reperfusion injury. Mammalian cells stably overexpressing BI-1 are protected against ER stress [2,3], and BI-1-deficient mice have increased infarct volumes after occlusion of the middle cerebral artery, a mouse stroke model, and increased sensitivity to tunicamycin-induced kidney toxicity [2]. The inhibitory effect of BI-1 on ER stress appears to be mediated via a direct interaction with inositol-requiring enzyme 1α (IRE1α), an ER resident serine/threonine protein kinase and endoribonuclease, which induces the expression of genes implicated in the unfolded protein response [4]. Lack of BI-1 therefore leads to a defective unfolded protein response and increased susceptibility to ER stress.

BI-1 also plays an important role in maintaining intracellular Ca^{2+} homeostasis. TMBIM6 knockout hepatocytes have an increased ER Ca^{2+} content [2], whereas overexpression of BI-1 causes reduced agonist-induced Ca^{2+} responses due to a reduced ER Ca^{2+} content [5]. A peptide corresponding to the semi-hydrophobic seventh transmembrane domain of BI-1 is capable of causing Ca^{2+} release from biological and artificial membranes, and this is abolished by the mutation of a single aspartic acid residue within this potential pore domain [6]. Also, full-length BI-1 with this mutation loses its ability to lower the ER Ca^{2+} content [6], suggesting that BI-1 is a Ca^{2+} leak channel in the ER membrane. Interestingly, decreases or increases in the intracellular pH shut down Ca^{2+} flux through the BI-1 channel but not in the pore-dead D213A mutant [7]). These observations are supported by a recent study characterizing the three-dimensional structure and pH-sensitive Ca^{2+}-flux properties of a bacterial homologue of BI-1, BsYetJ [8]. BsYetJ possesses a di-aspartyl pH sensor in its C-terminal pore domain (Asp171–

☆ This article is part of a Special Issue entitled: 13th European Symposium on Calcium. Guest Editors: Jacques Haiech, Claus Heizmann and Joachim Krebs.

* Corresponding author at: Department of Neurology, Johannes Gutenberg University Medical Center Mainz, Langenbeckstr. 1, Mainz D-55131, Germany, Tel.: +49 6131 17 2695; fax: +49 6131 17 5967.
E-mail address: axel.methner@gmail.com (A. Methner).

http://dx.doi.org/10.1016/j.bbamcr.2015.03.002
0167-4889/

Asp195), which corresponds to two aspartate residues in the pore domain of BI-1 (Asp188–Asp213). We therefore recently proposed a homology model of BI-1 and BsYetJ where the pore can be open (neutral pH), open and sealed (acidic pH) or closed (basic pH) depending on the cytosolic pH, explaining the bell-shaped effects of pH on Ca^{2+} flux mediated by BI-1 [9].

BI-1 is the founding member of a family consisting of a total of six BI-1-like proteins that have been described based on a signature pattern (Prosite PDOC00957) corresponding to a region that starts with the beginning of the third transmembrane domain and ends in the middle of the fourth: G – *x*(2) – [LIVM] – [GC] – P – *x* – [LI] – *x*(4) – [SAGDT] – *x*(4,6) – [LIVM](2) – *x*(2) – A – *x*(2) – [MG] – T – *x* – [LIVM] – *x* – F. These BI-1 family proteins have been identified in several instances by different groups and were given a wide variety of descriptive names. The nomenclature accepted by the HUGO gene nomenclature committee for this gene family is *TMBIM* (transmembrane BAX inhibitor motif containing) *1-6* with *BI-1* being *TMBIM6*. This nomenclature will be used for the remainder of the manuscript.

TMBIM1 (also known as RECS1, PP1201, LFG3, MST100, MSTP100) is a 35 kDa protein predicted to contain seven transmembrane domains located in endosomal/lysosomal membranes and ubiquitously expressed in brain, heart, lung, liver, kidney, stomach, intestine, ovary, uterus, skeletal muscle, skin, adipose tissue, but not in the thymus, spleen or testis [10]. TMBIM1/RECS1 plays a protective role in vascular remodeling and its deficiency induces susceptibility to cystic medial degeneration in aged mice [10]. TMBIM1/PP1201 also protects against Fas-mediated apoptosis by reducing Fas expression on the cell surface [11].

TMBIM2 (also known as NMP35, LFG, FAIM2, LFG2, NGP35, KIAA0950) is a 35 kDa protein also predicted to contain seven transmembrane helices. Intracellularly, TMBIM2 is located in the ER and in the Golgi apparatus as well as in lipid raft microdomains of the plasma membrane [12,13]. TMBIM2/NMP35 is predominantly expressed in the nervous system [14], most prominently in dendritic processes and in a subset of synapses at the postsynaptic membrane and density [15]. TMBIM2/LFG protects from cell death induced by the FAS ligand, but not by TNFα [12,13], and downregulation of endogenous TMBIM2/LFG by small interfering RNA increases sensitivity of neuronal cells to Fas ligand-induced cell death [12]. The lack of TMBIM2/FAIM2 increases caspase-associated cell death and stroke volume after cerebral ischemia in vivo [16].

TMBIM3 (also known as LFG1, HNRGW, NMDARA1, MGC99687, GRINA, GBP) is a 41 kDa protein predicted to have seven transmembrane helices first identified by expression cloning of a rat brain library based on immunoreactivity to an antibody against the glutamate-binding protein, a part of an NMDA-receptor-associated complex [17]. It was also identified as one out of 28 genes preferentially expressed beneath the marginal zone of the developing cerebral cortex of mice [18]. TMBIM3/GRINA is upregulated during ER stress and protects against ER stress-mediated cell death via a mechanism that involves TMBIM6 and IP_3Rs [19].

TMBIM4 (also known as GAAP, S1R, LFG4, ZPRO, CGI-119) is a 27 kDa protein predicted to contain seven transmembrane domains. TMBIM4/GAAP is expressed in many human tissues such as the heart, brain, placenta, lung, liver, skeletal muscle, kidney, pancreas, spleen, thymus, prostate, testis, ovary, small intestine and colon. Intracellularly, it is localized in membranes of the ER and Golgi apparatus. It was first identified in humans as GAAP with a highly conserved counterpart found in the vaccinia virus. The function of GAAP most closely resembles that of TMBIM6; human GAAP overexpression inhibits apoptosis triggered by intrinsic and extrinsic stimuli [20] and reduces histamine-induced Ca^{2+} release from intracellular stores by lowering the Ca^{2+} content of these stores and decreasing the efficacy of IP_3 [21].

TMBIM5 (also known as GHITM, MICS1, DERP2, My021, PTD010, HSPC282, FLJ26584, DKFZp566C0746) is a 37 kDa protein predicted to contain eight transmembrane domains. TMBIM5/GHITM is expressed ubiquitously in most tissues but less in the intestine and thymus [22]. Cleavage of a proposed N-terminal signal peptide results in its mature form in vivo [22]. TMBIM5/MICS1 appears to reside in the inner

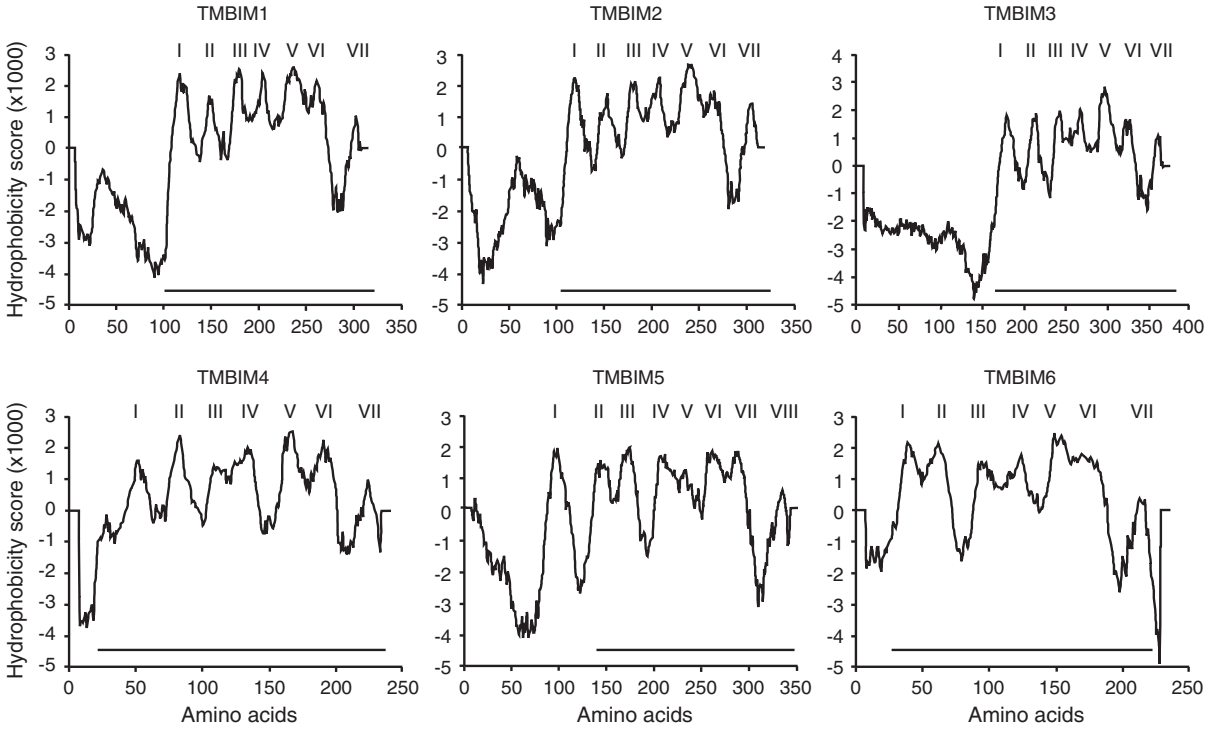

Fig. 1. The secondary protein structure of the TMBIM family. TMBIM1-6 all have at least 7 transmembrane domains, and the last domain is always much less hydrophobic than the others. Hydrophobicity plots of TMBIM1-6 were generated by TMpred. Putative transmembrane domains are indicated by roman numerals. The TMBIM6 homology domain is indicated by a horizontal line.

mitochondrial membrane and its downregulation results in the maintenance of the normal mitochondrial network and disorganization of cristae failing [23]. TMBIM5/MICS1 downregulation induces a rapid release of pro-apoptotic proteins from the mitochondria during apoptosis, whereas its overexpression induces a stabilization of cytochrome *c* at the inner membrane, irrespective of the permeabilization of the outer membrane during apoptosis [23].

In this work, we first studied the primary structure, phylogenetic relation and hydrophobicity of all mammalian TMBIM family proteins and BsYetJ. This revealed two groups of very similar structure and a complete conservation of the di-aspartyl sensor, suggesting comparable functions in the maintenance of intracellular Ca^{2+} homeostasis. We then compared tissue expression, intracellular localization and the effects on intracellular Ca^{2+} homeostasis of these proteins in parallel experiments.

2. Materials and methods

2.1. Cloning of TMBIM1-6 and generation of stable cell lines

TMBIM1-6 expressing HT22 cells were generated with the PiggyBac transposon system. cDNA sequences of TMBIM1-6 were generated by PCR and inserted into the pPB-CAG-EBNXN vector (obtained via the Sanger institute), N-terminally tagged with a hemagglutinin (HA) epitope and C-terminally followed by an internal ribosomal entry site (IRES) followed by the yellow fluorescent protein Venus. In TMBIM5-

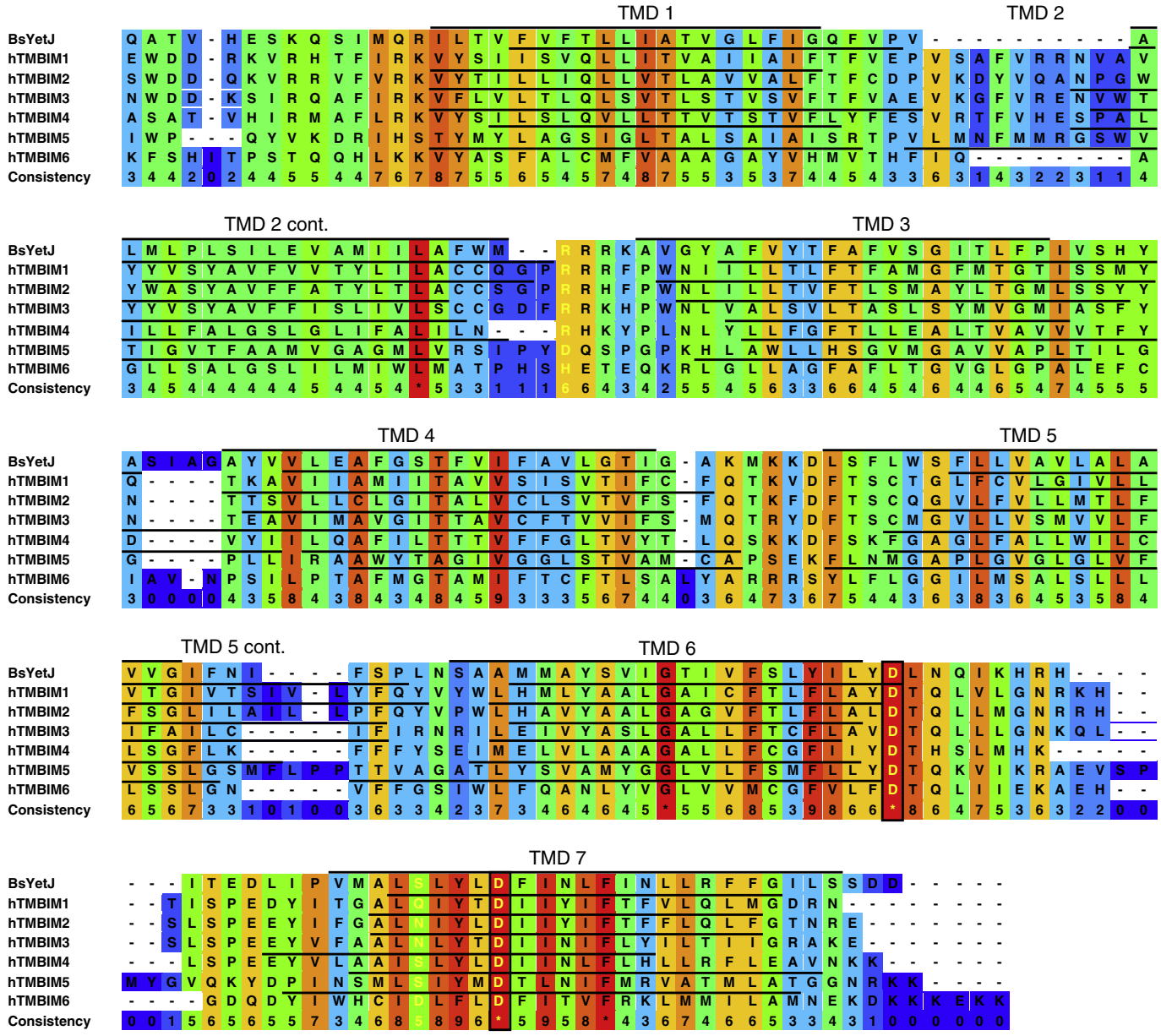

Fig. 2. Alignment of TMBIM proteins with the bacterial TMBIM6 ortholog BsYetJ. Multiple protein sequence alignment of the TMBIM protein family and the bacterial homologue BsYetJ was performed using PRALINE with the BLOSUM62 scoring matrix. The colors indicate the least conserved (blue) to the most conserved residues (red). Non-aligning N-termini of each protein were removed. Key residues previously shown to be important in gating pH-dependent Ca^{2+} leak by BsYetJ and putative corresponding residues in TMBIM6/BI-1 (H78, D188, D209 and D213) are shown in yellow. Note that only residues corresponding to D188 and D213 in TMBIM6 are strictly conserved across all proteins. Transmembrane domains (TMD) according to TMpred prediction are indicated by black lines.

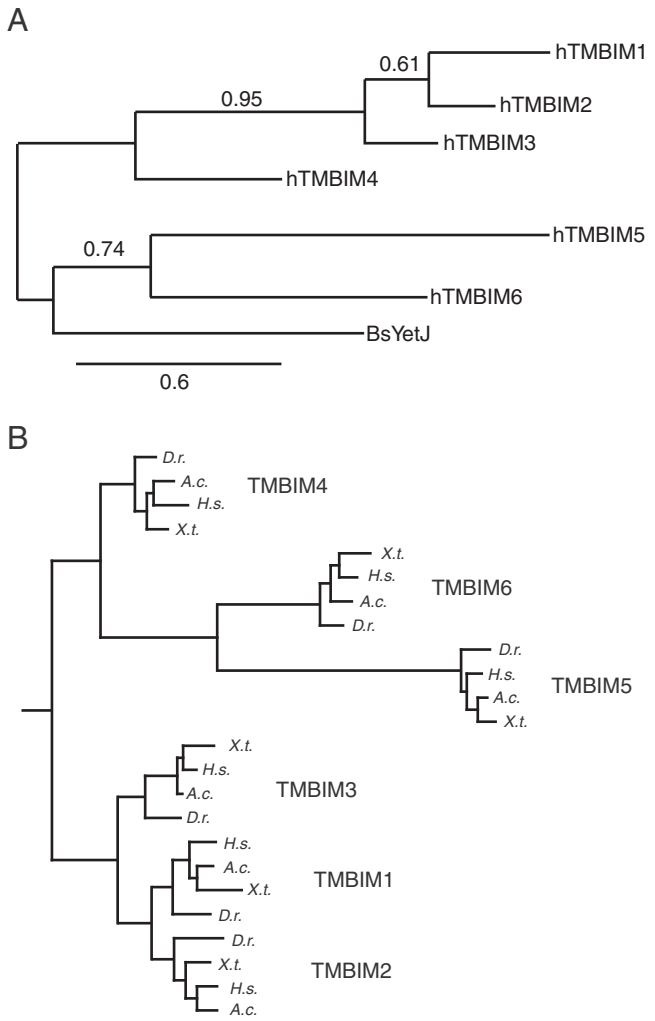

Fig. 3. TMBIM proteins share a common structure and fall into two separate groups. (A) Phylogenetic analysis of the sequence alignment of the TMBIM family and the bacterial homologue BsYetJ shows that BsYetJ is closest related to TMBIM5 and TMBIM6. The branch support values are indicated above the branches. (B) TMBIM6 clusters together with TMBIM5 and TMBIM4 and TMBIM1 clusters together with TMBIM2 and TMBIM3. TMBIM1 and TMBIM2 are the two most closely related proteins. TMBIM6 and TMBIM5 are more closely related to each other than to TMBIM4. Both phylogenetic trees were created using the Maximum Likelihood algorithm with the BLOSUM62 substitution matrix and 100 bootstrap trials.

mCherry, mCherry was cloned in frame C-terminally to TMBIM5. Each of these constructs was co-transfected in a ratio of 1:4 with a plasmid encoding a transposase into HT22 cells using Lipofectamine 2000 (Invitrogen) according to the manufacturer's protocol. The cDNA constructs, flanked by PiggyBac transposon sites, were stably inserted into the genome and 48 h after transfection Venus-positive cells were selected on a MoFlo XDP (Beckman-Coulter) cell sorter. After three to four repeated rounds of cell sorting, approximately 99% of cells were positive for Venus fluorescence and considered as stably transfected. Successful expression was confirmed by immunoblotting using an α-HA antibody (Sigma H6908, 1:2000).

2.2. Phylogenetic analysis and bioinformatic analysis

Multiple sequence alignment focusing on amino acid conservation was performed using the online tool PRALINE using the Blosum62 scoring matrix with default settings [24]. Alignments were preprocessed using PSI-BLAST with 3 iterations and an E-value cutoff of 0.01 [25]. The phylogenetic tree was constructed using the online tool phylogeny.fr [26]. In short, the tool aligns the sequences using MUSCLE (3.7) with default settings [27]. After alignment, ambiguous regions were removed by Gblocks (v0.91b) and reconstructed in a phylogenetic tree using the maximum likelihood method in PhyML (v3.0 aLRT). Graphics were created using TreeDyn (v198.3). The multiple sequence alignment of TMBIMs across species was created using MAFFT version 6 using the E-INS-i setting and the alignment trimmed with JalView 2.5 at a cutoff value of 85% gaps. For the analysis of the secondary structure of the TMBIM family, the amino acid sequence of each TMBIM protein family member was entered as plain text into the "Prediction of Transmembrane Regions and Orientation" (TMpred) application (ExPASy), and the prediction graphic of the preferred model with the highest score was chosen. The presence of signal peptides was evaluated with SignalP 4.0 [28] and of mitochondrial targeting sequences with MitoProt II [29].

2.3. Expression analysis

Wild-type C57/BL6 animals were sacrificed, and RNA was harvested from tissue samples with the ZN RNA Mini Prep Kit (ZYMO Research) according to the manufacturer's protocol. RNA was transcribed to

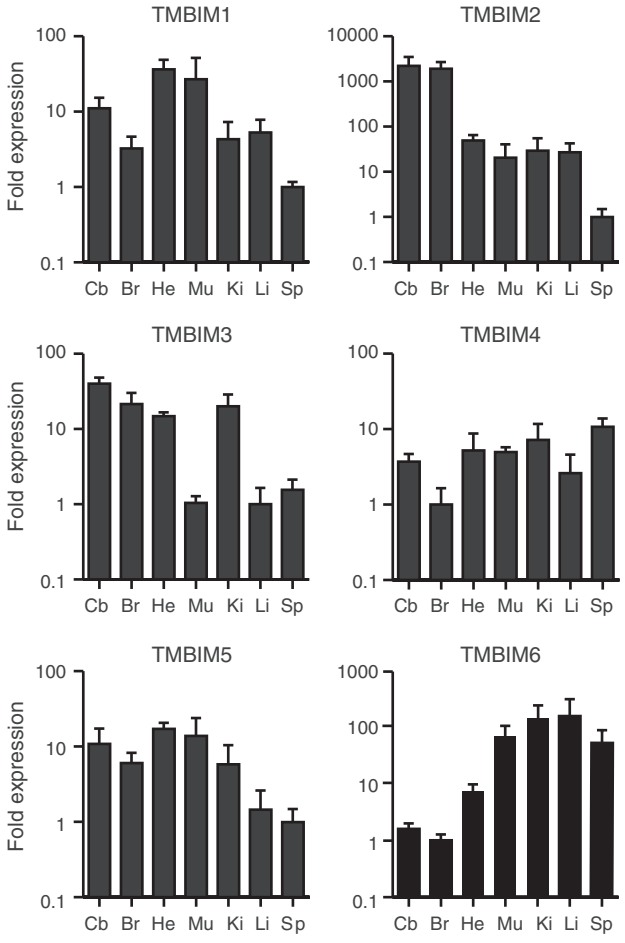

Fig. 4. Tissue expression of TMBIM family members. TMBIM1 is mainly expressed in the heart and in muscle and TMBIM2 and TMBIM3 are mostly found in the central nervous system where TMBIM6 is least expressed. TMBIM4 and TMBIM5 are relatively evenly distributed throughout the tissues. Expression of TMBIM1-6 as assessed by quantitative PCR in various tissues shown as the mean fold ± SEM from 3 to 6 mice per protein measured in triplicate. The fold was calculated with the $2^{-[delta][delta]Ct}$ method and was normalized to the tissue with the lowest expression.

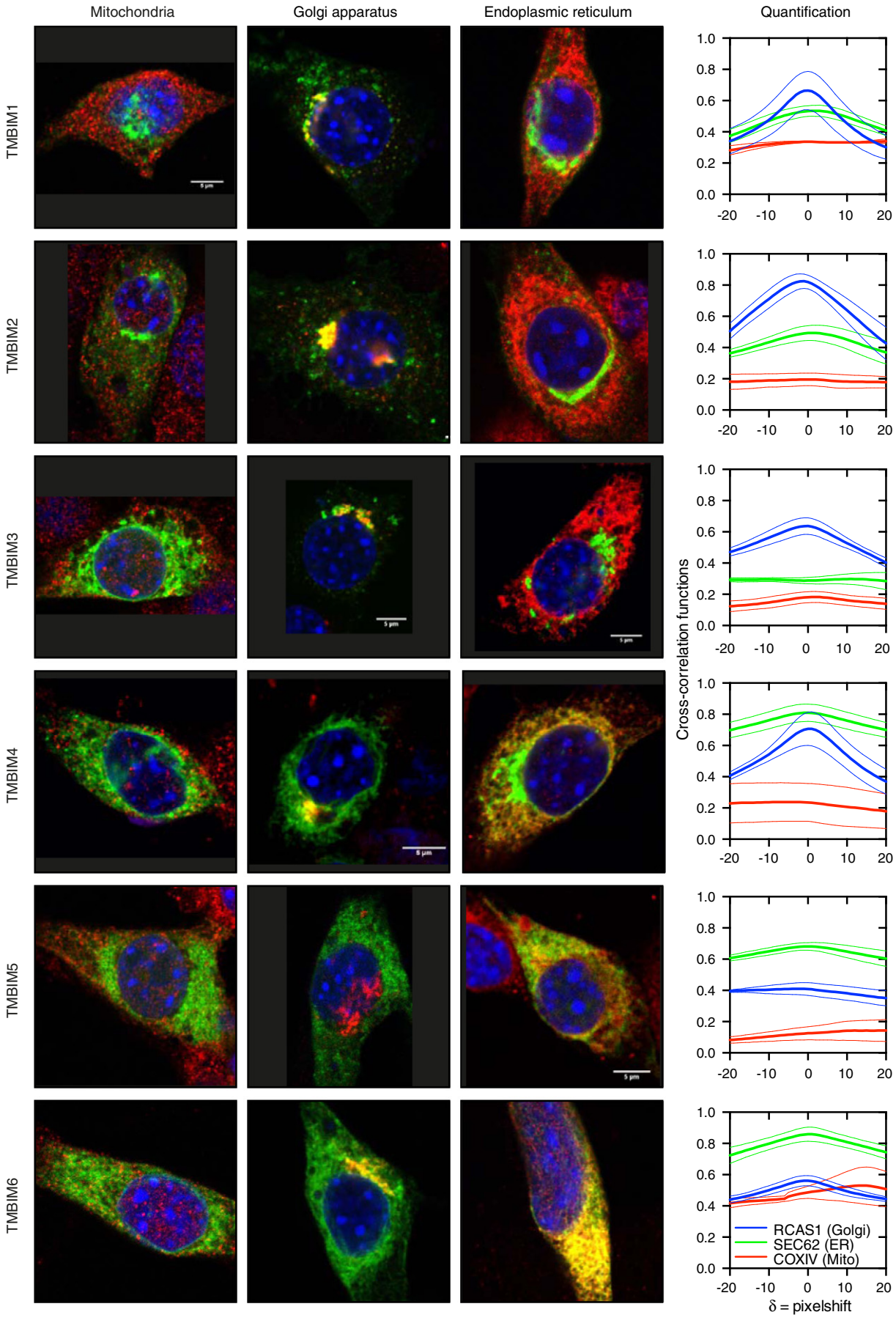
Mitochondria
Golgi apparatus
Endoplasmic reticulum
Quantification
TMBIM1
TMBIM2
TMBIM3
TMBIM4
TMBIM5
TMBIM6
Cross-correlation functions
1.0
0.8
0.6
0.4
0.2
0.0
-20
-10
0
10
20
RCAS1 (Golgi)
SEC62 (ER)
COXIV (Mito)
δ = pixelshift

cDNA with the High Capacity cDNA Reverse Transcription Kit (Applied Biosystems) using 2 μg of RNA. Quantitative PCR (qPCR) was employed to measure DNA levels in a 7500 Real Time System (Applied Biosystem), and the Universal Probe Library by Roche was used with the following primers: TMBIM1 forward: 5′-CAATGCCCATGAACTACGG-3′, TMBIM1 reverse: 5′-CCAGGACGAAAGCTGTCACT-3′, TMBIM2 forward: 5′-CCAC GCGGTCTATGCTGTA-3′, TMBIM2 reverse: 5′-CCATCAGCAACTGGGTAT CA-3′, TMBIM3 forward: 5′-CCGCATCCTGGAGATTGTAT-3′, TMBIM3 reverse: 5′-TGCTTGTTCCCCAGGAGTAG-3′, TMBIM4 forward: 5′-ACCTCT TCCTGCACCTGTTG-3′, TMBIM4 reverse: 5′-TCTCTGAACACTGCTCGGTT AC-3′, TMBIM5 forward: 5′-CTTGGAACCATCAATGGAAAA-3′, TMBIM5 reverse: 5′-AGAGCGCTCCAAGACCAAC-3′, TMBIM6 forward: 5′-GGGC CTATGTCCAGTGGT-3′, TMBIM6 reverse: 5′-CCATCAGCCAAATCATCA AG-3′. HPRT was used as an endogenous housekeeping gene. Fold expression was calculated with the $2^{-[delta][delta]Ct}$ method, and the expression of each protein was normalized to the tissue with the lowest fold.

2.4. Immunofluorescence

HT22 cells were plated in six-well tissue culture plates and grown for 24 h. Cells were then transiently transfected with the pPBCAG:HA-POI-IRES-Venus plasmids carrying the various TMBIM proteins using Attractene Transfection Reagent (Qiagen). After 24 h incubation, 75,000 cells were seeded on 12 mm coverslips and were grown for another 24 h. Cells were then washed with DPBS (Sigma-Aldrich) and fixed with 4 % paraformaldehyde for 20 min at 4 °C. Afterward, the cells were washed four times with DPBS (+0.1 M Glycin and 4 mM $MgCl_2$) for 5 min and then permeabilized and blocked with PSS (1x DPBS, 5% FCS, 0.1% Saponin) for 1 h at room temperature. Cells were incubated with the indicated primary antibodies (rabbit COXIV (1:750, Cell Signaling); rabbit RCAS1 (D2B6N, 1:100, Cell Signaling), mouse HA-Tag (6E2, Alexa Fluor 488 conjugate, 1:400, Cell Signaling), rabbit Sec62, (1:500, kind gift from Prof. Zimmermann, Universität des Saarlandes) in PSS overnight at 4 °C. After washing twice with PSS for 15 min, cells were incubated with the secondary antibody goat anti-rabbit Alexa568 (1:500, Milipore) for TMBIM 1-6 or goat anti-rabbit Alexa647 (1:1000, Invitrogen) for TMBIM5-mCherry in PSS for 1 h at 4 °C and washed three times with PSS for 5 min. The cell nuclei were stained with DAPI (Life Technologies) for 10 min and washed again twice with PSS. Coverslips were removed from the culture plate, washed with Aqua dest. and fixed on a microscope slide with mounting medium (Dako). Images were taken on a confocal microscope (SP5, Leica). Co-localization was quantified with the JACoP software (ImageJ) and the van Steensel approach [30].

2.5. Immunoblotting

HT22 cells were lysed in ice-cold RIPA buffer (Invitrogen) containing mini complete protease inhibitor cocktail (Roche) and centrifuged for 30 min at 16,000 g. Protein concentrations were determined using the bicinchoinic acid assay protein quantification kit (Interchim), samples were incubated for 10 min with 5x SDS loading dye with 8 M UREA. Fifty micrograms of each sample was loaded on polyacrylamide gels (Thermo Fisher Scientific), transferred onto nitrocellulose membranes with the iBlot System (Invitrogen) and blocked in 3% nonfat dry milk in PBS containing 0.5% Tween-20 (PBS-T). The membranes were incubated at 4 °C overnight with primary antibodies diluted 1:3000 for Anti-HA (ab9112, 1:3000, Abcam), Anti-Actin (MAB1501, clone C4, 1:4000, Millipore) or Anti-RFP (5 F8, 1:1000, Chromotek). Anti-mouse, anti-rabbit IgG (Fc) or Anti-rat infrared fluorescence conjugated secondary antibodies (Licor, 1:30.000) were added following washing with PBS-T and incubated for 1 h at RT. The membranes were scanned for infrared fluorescence at 680 and 800 nm using the Odyssey system (Licor).

2.6. Cytosolic Ca^{2+} measurements using Fura2

Fura2 Ca^{2+} imaging experiments were conducted on a BD Pathway 855 High Content Imaging System (BD Biosciences). HT22 cells were seeded in a density of 5000 cells/well on 96-well imaging plates (BD Bioscience) for 24 h and loaded with 5 μM Fura2-AM (Molecular Probes) in HBSS at 37 °C for 20 min prior to the experiment. Measurement was performed with excitation at 340 nm and 380 nm for radiometric analysis, and pictures were taken with a delay of 5 s. After baseline recording, ER Ca^{2+} stores were depleted in EGTA buffer (Ca^{2+}-free HBSS supplemented with 0.5 mM EGTA, 20 mM HEPES, 1 mM $MgCl_2$ and 1 g/l Glucose) with 2 μM thapsigargin for 8 min. Each cell type was measured at least three times and analyzed with Attovision 1.7.1.0 (BD Bioscience). Calibration was performed after each measurement, and Fura2 values were converted into absolute Ca^{2+} concentrations by the formula where the $k_d = 224$ nM, the min*Ratio* was measured in EGTA, max*Ratio* was measured in 20 mM Ca^{2+} and max380 and min380 represent the maximum and minimum values at 380 nm.

2.7. Statistical analysis

Data were analyzed as mean ± SEM and the statistical significance using two-tailed *t*-tests or analysis of variance (ANOVA) with Tukey's multiple comparison test as indicated.

3. Results

3.1. TMBIM proteins share a common structure and fall into two separate groups

We started by comparing the secondary protein structure of the human TMBIM family using TMpred, an algorithm that makes predictions about potential membrane-spanning regions and their orientation. This revealed a remarkably similar structure in all family members with at least seven domains with high hydrophobicity and an N-terminus of different lengths. Of note, in all TMBIM proteins, the last transmembrane domain is less or semi-hydrophobic as reported for TMBIM6 [6] and TMBIM4 [31]. These studies favored a six-transmembrane domain model with a putative reentrant loop at the C terminus and both termini located in the cytosol for these two proteins. Only TMBIM5, the only family member reported to have an N-terminal signal sequence that is cleaved in order to ensure proper protein expression and function [22], contains an additional transmembrane domain of significant hydrophobicity preceding the TMBIM6 homology region (Fig. 1). This domain, however, starts at amino acid 82 and likely does not serve as a signal peptide sequence, an aspect that is studied in more detail in this manuscript. We next aligned the sequences of all TMBIM proteins with the bacterial TMBIM6 ortholog BsYetJ using the online tool PRALINE. This

Fig. 5. Group-specific expression in the Golgi apparatus or the ER. TMBIM1-3 mainly co-localized with a Golgi apparatus marker and TMBIM4-6 with an ER marker. None of the N-terminally tagged TMBIM family member co-localized with mitochondria. HT22 cells were transiently transfected with HA-tagged TMBIM 1-6 and stained with primary antibodies against HA and either COXIV (mitochondria), RCAS1 (Golgi apparatus) or Sec62 (ER). FITC-labeled secondary antibodies against HA (green) and Cy3-labeled secondary antibodies against COX IV, RCAS1 and Sec62 (red) were used to assess intracellular localization of TMBIM1-6 with confocal microscopy. The scale bar corresponds to 5 μm. The JACoP software with the van Steensel approach was employed to quantify co-localization.

revealed a strong conservation of the first five amino acids preceding transmembrane domain (TMD) 1 and the TMD 6 and 7, respectively, 2 and 7/8 in TMBIM5. All proteins contain the completely conserved di-aspartyl pH sensor identified in BsYetJ [8]. Besides this, only two other residues were completely conserved in all proteins: a leucine in TMD 2 and a phenylalanine in TMD 7 (Fig. 2). We next generated a phylogenetic tree to clarify the relationship of the TMBIM family members to BsYetJ, which revealed that TMBIM6 is the closest relative to this ancestral protein (Fig. 3A). To more clearly delineate the relationship of the TMBIM family members to each other, we then constructed a phylogenetic tree using a completely unrelated TMD protein as an outlier and 100 bootstrap trials. We also chose orthologs of TMBIM1-6 from four evolutionarily separated vertebrates (*Homo sapiens*, *Anolis carolinensis*, *Xenopus tropicalis* and *Danio rerio*) to avoid species-specific changes or artifacts. The resulting phylogenetic tree clearly separated the six TMBIM family members and revealed two separate clades: group I (TMBIM1, TMBIM2 and TMBIM3) and group II (TMBIM4, TMBIM5 and TMBIM6). Within the groups, TMBIM1 and 2 and TMBIM5 and 6 clustered together (Fig. 3B). In summary, these results suggest a close homology of all TMBIM family members and reveal that the previously identified di-aspartyl pH sensor is conserved among all TMBIM proteins.

3.2. Tissue expression of TMBIM family members

The hydrophobic nature of the TMBIM family renders the generation of specific antibodies difficult. Despite considerable efforts, no functional antibodies that can distinguish between TMBIM6 deficient, and wild-type tissues are currently available (see supplementary data in [7]). We therefore used quantitative RT-PCR to quantitate the expression of the TMBIM family members in a comparable manner in the cerebellum, brain, heart, femoral muscle, kidney, liver and spleen. The housekeeping gene hypoxanthine-guanine phosphoribosyltransferase (*hprt*) served as an endogenous control, and the expression of each transcript was normalized to the tissue with the lowest expression. This revealed that TMBIM1 has its highest expression in the two muscle tissues, TMBIM2 and TMBIM3 in the two tissues from the central nervous system, TMBIM4 and TMBIM5 are rather ubiquitously expressed and TMBIM6 predominantly in skeletal muscle, the kidney, liver and spleen (Fig. 4).

3.3. Group-specific expression in the Golgi apparatus or the ER in HT22 cells

A number of different intracellular locations for each TMBIM family member were proposed mainly based on bioinformatic predictions. We decided to compare the intracellular localization of all family members in a comparable and quantitative manner and transiently transfected HT22 cells with N-terminally HA-tagged TMBIM1-6, which were then stained with an α-HA antibody and antibodies against the Golgi marker protein receptor binding cancer antigen expressed on SiSo cells (RCAS1) [32], the ER marker protein SEC62 [33] and the mitochondrial protein cytochrome *c* oxidase IV (COXIV) [34]. Co-localization was quantified by the van Steensel cross-correlation function and the Pearson coefficient [30]. This proved an interesting dichotomy in that group I (TMBIM1-3) showed a predominant localization in the Golgi apparatus and group II (TMBIM4-6) in the endoplasmic reticulum (Fig. 5). Because of the reported mitochondrial localization of TMBIM5 [23] and the fact that its secondary structure differs from the other family members by the presence of an additional transmembrane domain preceding the TMBIM6 homology domain (Fig. 1), we decided to study this protein in more detail. Yoshida et al. [22] reported the presence of an N-terminal signal sequence, which we could not verify using the SignalP 4.0 detection method [28] (Fig. 6A). We, however, noted an enrichment of arginine, leucine, serine and alanine residues (shown in blue in Fig. 6A), a net charge of +18 and a predominance of basic amino acids in the TMBIM5 N-terminus. These are all characteristics of a mitochondrial targeting sequence [29] and an analysis with MitoProt II indeed indicated the presence of a potential cleavage site at position 57 of TMBIM5 (Fig. 6A). In the experiments described above, we tagged TMBIM5 with the 11-amino acid HA tag at its N-terminal end and used an antibody against this tag to determine the subcellular localization. Because we observed a band of the predicted size by immunoblotting this means that at least a part of TMBIM5 remains uncleaved and that this uncleaved TMBIM5 resides in the ER whereas cleaved TMBIM5 could reside in mitochondria. To distinguish between these two possibilities, we now cloned the red fluorescent mCherry protein in frame with the C terminus of TMBIM5 and studied the subcellular localization by co-localizing mCherry fluorescence with the organelle markers. In comparison to the N-terminally tagged protein, this revealed a reduced localization in the ER, an absent localization in the Golgi apparatus and a significant co-localization with the mitochondrial marker protein cytochrome *c* oxygenase IV (Fig. 6B). Also, when we immunoblotted transiently transfected TMBIM5-mCherry and stained with an α-mCherry antiserum, we observed two distinct bands of equal density but only one band when stained with an α-HA antiserum (Fig. 6C). This means that TMBIM5 can indeed be cleaved after the predicted mitochondrial targeting signal and translocate to mitochondria.

3.4. Profound effects of TMBIM 1-6 on the intracellular Ca^{2+} homeostasis in HT22 cells

Ca^{2+} is an important signaling molecule in the cytosol of virtually all cell types and several members of the TMBIM protein family, especially TMBIM6, have been reported to play a role in the control of intracellular Ca^{2+} homeostasis. We investigated the effect of each family member on intracellular Ca^{2+} by stably overexpressing HA-tagged TMBIM1-6 in HT22 cells. The expression of each protein was confirmed by immunoblotting (Fig. 7A). Ca^{2+} kinetics were measured in a high-throughput microscope which allows simultaneous measurement of several hundred cells independently. The ER Ca^{2+} content was measured by applying thapsigargin, an irreversible inhibitor of the SERCA pumps in the ER membrane, causing immediate Ca^{2+} efflux from the ER. In the presence of the extracellular Ca^{2+} buffer, Ca^{2+} influx from the extracellular medium is prevented and the thapsigargin-releasable Ca^{2+} in the cytosol is solely originating from the ER Ca^{2+} stores. The TMBIM-expressing HT22 cells were compared to HT22 cells that only expressed the empty vector. Fig. 7B shows the combined Ca^{2+} traces of each cell line and Fig. 7C a quantitative analysis of the baseline cytosolic [Ca^{2+}] and the peak [Ca^{2+}] reached after addition of thapsigargin. In these experiments, we examined one cell line after another and always compared against the control cell line explaining the higher number of analyzed cells. This revealed that all TMBIM family members reduced the ER Ca^{2+} content and all but TMBIM5 also reduced the basal Ca^{2+} concentration in the cytosol.

4. Discussion

This is the first work systematically describing the relationship, secondary structure, tissue expression, intracellular localization and effects on cellular Ca^{2+} homeostasis of the TMBIM protein family sharing the evolutionary conserved motif UPF0005. All family members are characterized by at least six transmembrane domains and an additional C-terminal domain that may serve as a reentrant loop, as previously proposed for TMBIM6 [6] and TMBIM4 [31]. Our phylogenetic analysis demonstrated two groups consisting of TMBIM1-3 on one hand and TMBIM4-6 on the other, which differ mainly in regard to intracellular localization. We could confirm that TMBIM1 [11], TMBIM2 [12] and TMBIM3 [19,35] are mainly located in the Golgi apparatus and to a lesser extent in the ER. TMBIM4 and TMBIM5 are more closely related to TMBIM6 and these three have a predominant localization in the ER. Gubser et al. [20] also found TMBIM4 primarily located in the ER and

partly in the Golgi apparatus in line with our results. Regarding TMBIM5, a previous study suggested that it is exclusively located in the mitochondria [23]. We indeed identified the presence of a mitochondrial targeting sequence in this protein leading to cleavage after residue 57 and therefore repeated our co-localization experiments using C-terminally tagged TMBIM5. This still demonstrated a predominant ER localization but also a substantial mitochondrial localization not present in the co-localization experiments with the N-terminal tag. We therefore assume that TMBIM5 can be localized at different organelles depending on the efficiency of cleavage that could be altered by the presence of the small HA tag at its N-terminus as suggested earlier [22]. It should be noted, however, that a bioinformatic analysis using PSORT II also suggested a predominant ER localization. Interestingly, a splice isoform of TMBIM5 (GenBank accession EAW80370.1) with 243 amino acids adding a novel N-terminus starting 10 amino acids before the TMBIM6 homology domain can be found in databases. Such a protein would most probably not localize to mitochondria. Finally, TMBIM6 was undoubtedly expressed in the ER in line with previous data using EGFP- [1,5] and mCherry-tagged [7] TMBIM6.

In line with Zhao et al., we detected the lowest expression of TMBIM1 in the spleen where it was below the detection limit of northern blotting. We observed the highest expression of TMBIM1 in the heart and in the skeletal muscle, followed by the cerebellum, which is similar to the expression pattern previously obtained by northern blotting [10]. Our results are also in line with previous observations from northern blotting [13,14], RT-PCR [12] and immunohistochemistry [15] that TMBIM2 is mainly expressed in the central nervous system. TMBIM3 was also found to be mainly expressed in the central nervous system and to a lower extent in the kidney by northern blotting and RT-PCR [35], supporting our own results which show a comparable expression pattern. TMBIM4 has been reported by PCR analysis to be ubiquitously expressed throughout all tissues with its lowest expression being in the brain [20], which exactly matches our results. Northern blot analysis showed that TMBIM5 is highly expressed in the brain, heart, liver kidney and muscle with lower expression in the intestines and in the thymus [22]. Our data support this analysis since we observed a similar expression pattern, although we measured a lower expression in the liver compared to the brain, heart and skeletal muscle. TMBIM6, also known as BI-1, is the best-characterized member of the TMBIM family yet. We were able to confirm its ubiquitous expression throughout the body [36–38] with the exception of the nervous system.

In line with the conserved overall structure and the homology with TMBIM6, we observed that the overexpression of each protein resulted in a decreased thapsigargin-releasable Ca^{2+} pool from the ER. A lowering effect on the ER Ca^{2+} content has been previously reported for TMBIM3 [19], TMBIM4 [21] and TMBIM6 [5]. Yet the impact of TMBIM1, TMBIM2 and TMBIM5 on intracellular Ca^{2+} homeostasis has not been reported before, but our data are now the first to indicate that these proteins indeed influence the Ca^{2+} handling of the ER. Westphalen et al. [5] transfected CHO cells with TMBIM6-EGFP and measured Ca^{2+} traces after ATP stimulation with the ratiometric Ca^{2+} dye Fura2-AM and the ER Ca^{2+} content after treatment with thapsigargin using the ER cameleon D1ER. Rojas-Rivera et al. stably

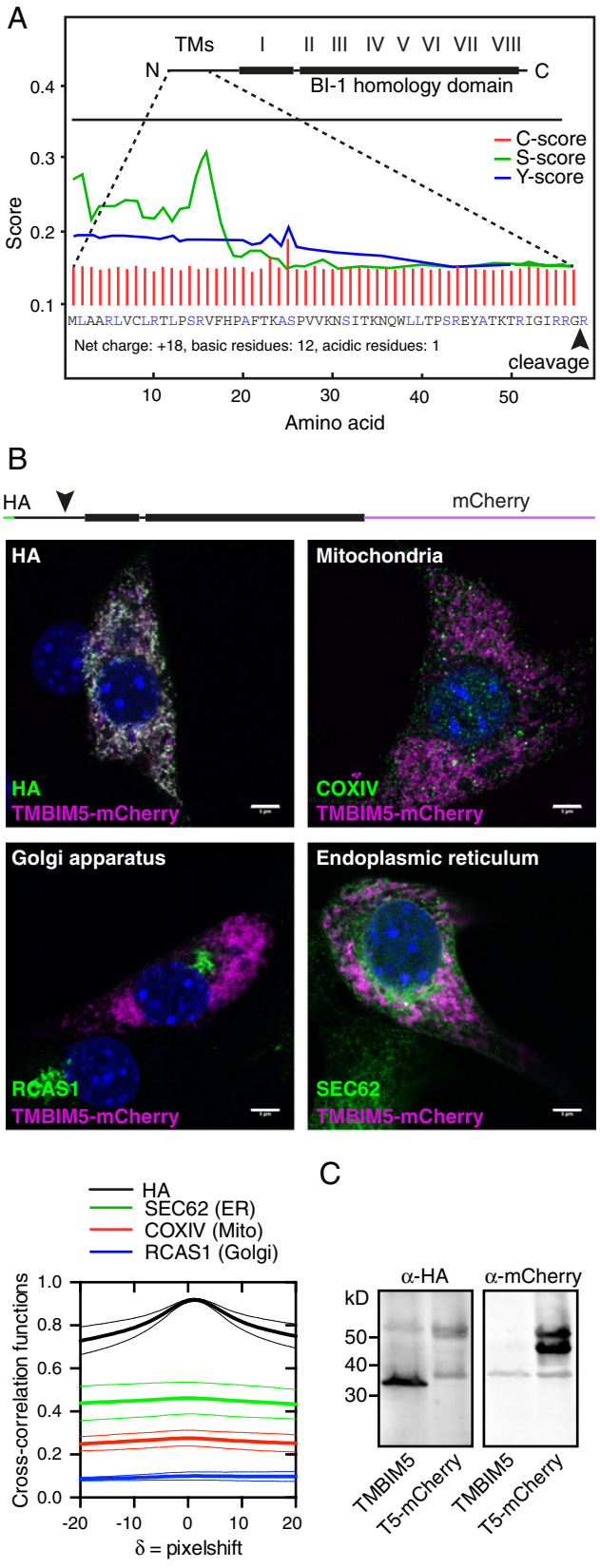

Fig. 6. Detailed analysis of the subcellular localization of TMBIM5. (A) TMBIM5 contains no signal peptide but a mitochondrial targeting sequence with a proposed cleavage after residue 57. The amino acid sequence was analyzed by SignalP 4.0 and MitoProt II. None of the scores reported by SignalP 4.0 (C, S, Y scores) reaches the threshold necessary for classification as signal peptide shown as horizontal line. However, the N-terminus possesses a net positive charge and 21 out of 57 residues typically found in mitochondrial targeting sequences (shown in blue). The predicted cleavage site is indicated by an arrow. (B) C-terminally mCherry-tagged TMBIM5 localizes to mitochondria and the ER. HT22 cells were transiently transfected with TMBIM5 tagged on both sides and stained with primary antibodies against HA and mCherry, or mCherry and either COXIV (mitochondria), RCAS1 (Golgi apparatus) or Sec62 (ER). FITC-labeled secondary antibodies against HA or the organelle markers (green) and Cy3-labeled secondary antibodies against mCherry (magenta) were used to assess intracellular localization with confocal microscopy. The scale bar corresponds to 5 μm. The JACoP software with the van Steensel approach was employed to quantify co-localization. (C) TMBIM5 is cleaved. HT22 cells were transiently transfected with HA-TMBIM5-mCherry and immunoblotted. The mCherry-stained blot reveals two bands corresponding to cleaved and uncleaved TMBIM5 whereas the HA-stained blots shows only a single band. Size is indicated.

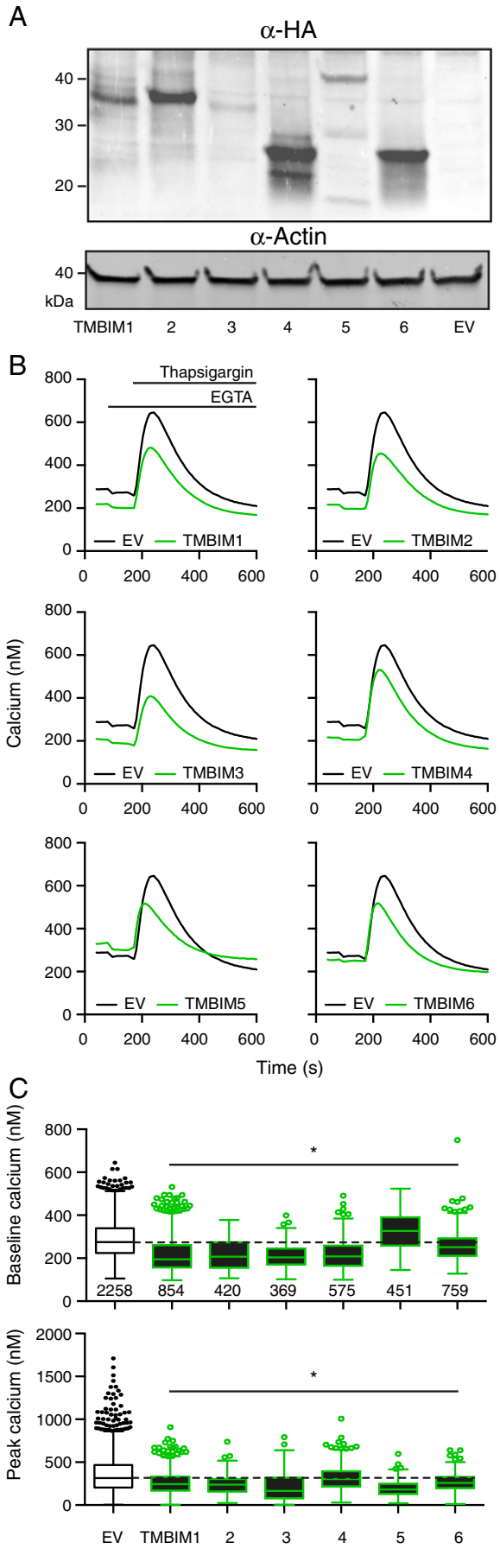

overexpressed TMBIM3-myc in mouse embryonic fibroblasts and measured Ca^{2+} release with Fluo4-AM after ATP stimulation [19]. HA-tagged TMBIM4 was stably overexpressed in U2OS cells, which were stimulated with histamine and Ca^{2+} was measured with Fura2-AM by de Mattia et al. [21]. In all cases, the overexpression of the TMBIM family members resulted in a decreased agonist-inducible Ca^{2+} pool, similarly to the reduced thapsigargin-releasable pool, which we observed after stably overexpressing TMBIM1-6 in HT22 cells. This property likely is not limited to mammalian TMBIM proteins since the overexpression of viral TMBIM4 has been shown to lower the ionomycin-releasable Ca^{2+} in cells [39]. However, it is important to note that the impact of TMBIM on agonist-induced Ca^{2+} release is not solely due to its impact on the filling state of the ER Ca^{2+} stores since several TMBIM family members (TMBIM3, TMBIM4 and TMBIM6) have been reported to interact with the IP3 receptor, an intracellular Ca^{2+}-release channel present at the ER Ca^{2+} stores. On one hand, TMBIM6 overexpression sensitizes IP3R to low [IP3] and thus promotes IP3-induced Ca^{2+} release in Ca^{2+}-flux assays performed in permeabilized cell systems [40]; on the other TMBIM3 [19] or TMBIM4 [21] overexpression suppressed IP3-induced Ca^{2+} release in these assays which could of course be also caused by the reduced ER Ca^{2+} content.

Whether the Ca^{2+} flux through all TMBIM family members is pH dependent remains to be investigated. The pH-dependent properties of TMBIM6 are due to a complex network of interactions with a prominent role for the di-aspartyl pH sensor (D188 and D213 of TMBIM6) conserved in all family members, but also on D209 and H78. At neutral pH, the D188, D209 and D213, which form the Ca^{2+}-permeable pore, are sufficiently negatively charged to allow Ca^{2+} flux. At more acidic pH (e.g. about pH 6), D188 and D213 become protonated (due to their relatively high p*K*a values) and prevent Ca^{2+} flux through the pore. At more basic pH, a hydrogen bond between H78 and D213 may be formed and thus alter the conformation, leading to closure of the Ca^{2+} pore (discussed in [9]). In contrast to D188 and D213 residues, which are conserved among all TMBIM family members, H78 and D209 are unique to TMBIM6. However, all other family members also contain a positively charged residue (namely R) at this position except TMBIM5, where it corresponds to a negatively charged residue (namely D). The importance of this residue for the function of the TMBIM family members awaits further investigation. It is interesting to note that all TMBIM family members except TMBIM5 caused a slight decrease in the basal cytosolic [Ca^{2+}], which matches an increased cytosolic Ca^{2+} content in TMBIM6 knockout splenocytes (own unpublished data). At this point, it is not clear what causes this and why TMBIM5 overexpression has the opposite effect. TMBIM5 differs from the other family members by the presence of a unique acidic (D) instead of a basic (H or R) residue near transmembrane domain 2, an additional transmembrane domain preceding the TMBIM6 homology domain and its unique localization in the mitochondrial membranes. This mitochondrial localization

Fig. 7. Profound effects of TMBIM 1-6 on the intracellular Ca^{2+} homeostasis. (A) Cells stably express HA-tagged TMBIM family members. HT22 cells were stably transfected with HA-tagged TMBIM1-6 or empty vector and expression was verified by immunoblotting. Actin was used as the loading control; size is indicated. (B) Each member of the TMBIM family, except for TMBIM5, lowered the baseline Ca^{2+} compared to cells transfected with the empty vector. Additionally, TMBIM1-6 lowered the thapsigargin-releasable pool. The traces show the calibrated absolute Ca^{2+} concentrations of each cell line compared to empty vector-transfected cells. Each cell line was measured at least three times and the total cell count is indicated in panel C. (C) Single-cell analysis of the Ca^{2+} traces shows that while TMBIM1-4 and TMBIM6 significantly but modestly lowered the basal cytosolic [Ca2+], TMBIM5 significantly increased it. Further, each TMBIM family member significantly decreased the ER Ca^{2+} pool when compared to empty vector-transfected cells. Fura2-AM-based Ca^{2+} traces were recorded with a high content imaging system. After baseline recording, extracellular Ca^{2+} was depleted by adding 2 mM EGTA. Then ER Ca^{2+} content was released through the addition of 2 μM thapsigargin. The box and whiskers plot represent the absolute Ca^{2+} values at baseline conditions as well as the maximum cytosolic Ca^{2+} concentrations as the mean ± SD. Data were analyzed with one-way ANOVA. *$P < 0.05$.

could alter the buffering capacity of the mitochondria and thereby alter the cytosolic Ca^{2+} levels.

The reduction of intracellular Ca^{2+} concentrations might impact the cell's susceptibility to apoptosis since Ca^{2+} is known to influence apoptosis pathways (reviewed in [41,42]). Ca^{2+} released from the ER can be taken up by the mitochondria, which is facilitated by the close proximity of these two organelles [43]. Although Ca^{2+} uptake by the mitochondria can activate oxidative metabolism and promote cell survival, dysregulated release of ER Ca^{2+} initiates programmed cell death by several mechanisms including mitochondrial Ca^{2+} overload, depolarization, ATP loss, generation of reactive oxygen species, and cytochrome *c* release (reviewed in [44]). The decreased ER and Golgi Ca^{2+} pool by the overexpressed members of the TMBIM family members might therefore correlate with their potential anti-apoptotic properties that has been recently reviewed elsewhere [45]. We were unfortunately not able to reliably measure cell death in our cell lines. This resulted primarily from very heterogeneous growth characteristics between the cell lines, also between empty vector-transfected cells and cells carrying the actual protein. It therefore remains to be investigated how the changes in the intracellular Ca^{2+} handling caused by the TMBIM family exactly relate to their anti-apoptotic properties.

Conflict of interest

The authors have no conflict of interest.

Traparency Document

The Transparency document associated with this article can be found, in the online version.

Acknowledgment

This work was supported by DFG ME1922/9-1 to Axel Methner. Support in the laboratory of Geert Bultynck was provided by the KU Leuven (OTSTRT1/10/044 and OT/14/101) and from the Research Foundation–Flanders (FWO; G.0571.12). We thank Darragh O'Neill for proofreading the manuscript. Confocal images were taken in the Core Facility Microscopy of the Institute of Molecular Biology (IMB) Mainz.

References

[1] Q. Xu, J.C. Reed, Bax inhibitor-1, a mammalian apoptosis suppressor identified by functional screening in yeast, Mol. Cell 1 (1998) 337–346.
[2] H.-J. Chae, H.-R. Kim, C. Xu, B. Bailly-Maitre, M. Krajewska, S. Krajewski, et al., BI-1 regulates an apoptosis pathway linked to endoplasmic reticulum stress, Mol. Cell 15 (2004) 355–366, http://dx.doi.org/10.1016/j.molcel.2004.06.038.
[3] B. Bailly-Maitre, C. Fondevila, F. Kaldas, N. Droin, F. Luciano, J.-E. Ricci, et al., Cytoprotective gene bi-1 is required for intrinsic protection from endoplasmic reticulum stress and ischemia-reperfusion injury, Proc. Natl. Acad. Sci. U. S. A. 103 (2006) 2809–2814, http://dx.doi.org/10.1073/pnas.0506854103.
[4] F. Lisbona, D. Rojas-Rivera, P. Thielen, S. Zamorano, D. Todd, F. Martinon, et al., BAX inhibitor-1 is a negative regulator of the ER stress sensor IRE1alpha, Mol. Cell 33 (2009) 679–691, http://dx.doi.org/10.1016/j.molcel.2009.02.017.
[5] B.C. Westphalen, J. Wessig, F. Leypoldt, S. Arnold, A. Methner, BI-1 protects cells from oxygen glucose deprivation by reducing the calcium content of the endoplasmic reticulum, Cell Death Differ. 12 (2005) 304–306, http://dx.doi.org/10.1038/sj.cdd.4401547.
[6] G. Bultynck, S. Kiviluoto, N. Henke, H. Ivanova, L. Schneider, V. Rybalchenko, et al., The C terminus of Bax inhibitor-1 forms a Ca2 + -permeable channel pore, J. Biol. Chem. 287 (2012) 2544–2557, http://dx.doi.org/10.1074/jbc.M111.275354.
[7] S. Kiviluoto, T. Luyten, L. Schneider, D. Lisak, D. Rojas-Rivera, K. Welkenhuyzen, et al., Bax Inhibitor-1-mediated Ca(2 +) leak is decreased by cytosolic acidosis, Cell Calcium 54 (2013) 186–192, http://dx.doi.org/10.1016/j.ceca.2013.06.002.
[8] Y. Chang, R. Bruni, B. Kloss, Z. Assur, E. Kloppmann, B. Rost, et al., Structural basis for a pH-sensitive calcium leak across membranes, Science 344 (2014) 1131–1135, http://dx.doi.org/10.1126/science.1252043.
[9] G. Bultynck, S. Kiviluoto, A. Methner, Bax inhibitor-1 is likely a pH-sensitive calcium leak channel, not a H +/Ca2 + exchanger, Sci. Signal. 7 (2014) pe22, http://dx.doi.org/10.1126/scisignal.2005764.
[10] H. Zhao, A. Ito, S.H. Kimura, N. Yabuta, N. Sakai, M. Ikawa, et al., RECS1 deficiency in mice induces susceptibility to cystic medial degeneration, Genes Genet. Syst. 81 (2006) 41–50.
[11] A shear stress responsive gene product PP1201 protects against Fas-mediated apoptosis by reducing Fas expression on the cell surface, 162011. 162–173, http://dx.doi.org/10.1007/s10495-010-0556-y.
[12] M. Fernández, M.F. Segura, C. Solé, A. Colino, J.X. Comella, V. Ceña, Lifeguard/neuronal membrane protein 35 regulates Fas ligand-mediated apoptosis in neurons via microdomain recruitment, J. Neurochem. 103 (2007) 190–203, http://dx.doi.org/10.1111/j.1471-4159.2007.04767.x.
[13] N.V. Somia, M.J. Schmitt, D.E. Vetter, D. Van Antwerp, S.F. Heinemann, I.M. Verma, LFG: an anti-apoptotic gene that provides protection from Fas-mediated cell death, Proc. Natl. Acad. Sci. U. S. A. 96 (1999) 12667–12672.
[14] B. Schweitzer, V. Taylor, A.A. Welcher, M. McClelland, U. Suter, Neural membrane protein 35 (NMP35): a novel member of a gene family which is highly expressed in the adult nervous system, Mol. Cell. Neurosci. 11 (1998) 260–273, http://dx.doi.org/10.1006/mcne.1998.0697.
[15] B. Schweitzer, U. Suter, V. Taylor, Neural membrane protein 35/Lifeguard is localized at postsynaptic sites and in dendrites, Brain Res. Mol. Brain Res. 107 (2002) 47–56.
[16] Fas/CD95 Regulatory Protein Faim2 Is Neuroprotective after Transient Brain Ischemia, 312011. 225–233, http://dx.doi.org/10.1523/JNEUROSCI.2188-10.2011.
[17] K.N. Kumar, N. Tilakaratne, P.S. Johnson, A.E. Allen, E.K. Michaelis, Cloning of cDNA for the glutamate-binding subunit of an NMDA receptor complex, Nature 354 (1991) 70–73, http://dx.doi.org/10.1038/354070a0.
[18] Identification of molecules preferentially expressed beneath the marginal zone in the developing cerebral cortex, 602008. 135–146, http://dx.doi.org/10.1016/j.neures.2007.10.006.
[19] D. Rojas-Rivera, R. Armisén, A. Colombo, G. Martínez, A.L. Eguiguren, A. Díaz, et al., TMBIM3/GRINA is a novel unfolded protein response (UPR) target gene that controls apoptosis through the modulation of ER calcium homeostasis, Cell Death Differ. 19 (2012) 1013–1026, http://dx.doi.org/10.1038/cdd.2011.189.
[20] A New Inhibitor of Apoptosis from Vaccinia Virus and Eukaryote, 32007. e17, http://dx.doi.org/10.1371/journal.ppat.0030017.
[21] F. de Mattia, C. Gubser, M.M.T. van Dommelen, H.-J. Visch, F. Distelmaier, A. Postigo, et al., Human Golgi antiapoptotic protein modulates intracellular calcium fluxes, Mol. Biol. Cell 20 (2009) 3638–3645, http://dx.doi.org/10.1091/mbc.E09-05-0385.
[22] T. Yoshida, S. Nagata, H. Kataoka, Ghitm is an ortholog of the Bombyx mori prothoracic gland-derived receptor (Pgdr) that is ubiquitously expressed in mammalian cells and requires an N-terminal signal sequence for expression, Biochem. Biophys. Res. Commun. 341 (2006) 13–18, http://dx.doi.org/10.1016/j.bbrc.2005.12.141.
[23] T. Oka, T. Sayano, S. Tamai, S. Yokota, H. Kato, G. Fujii, et al., Identification of a novel protein MICS1 that is involved in maintenance of mitochondrial morphology and apoptotic release of cytochrome *c*, Mol. Biol. Cell 19 (2008) 2597–2608, http://dx.doi.org/10.1091/mbc.E07-12-1205.
[24] S. Henikoff, J.G. Henikoff, Amino acid substitution matrices from protein blocks, Proc. Natl. Acad. Sci. U. S. A. 89 (1992) 10915–10919.
[25] V.A. Simossis, J. Kleinjung, J. Heringa, Homology-extended sequence alignment, Nucleic Acids Res. 33 (2005) 816–824, http://dx.doi.org/10.1093/nar/gki233.
[26] A. Dereeper, V. Guignon, G. Blanc, S. Audic, S. Buffet, F. Chevenet, et al., Phylogeny.fr: robust phylogenetic analysis for the non-specialist, Nucleic Acids Res. 36 (2008) W465–W469, http://dx.doi.org/10.1093/nar/gkn180.
[27] R.C. Edgar, MUSCLE: multiple sequence alignment with high accuracy and high throughput, Nucleic Acids Res. 32 (2004) 1792–1797, http://dx.doi.org/10.1093/nar/gkh340.
[28] T.N. Petersen, S. Brunak, G. von Heijne, H. Nielsen, SignalP 4.0: discriminating signal peptides from transmembrane regions, Nat. Methods 8 (2011) 785–786, http://dx.doi.org/10.1038/nmeth.1701.
[29] M.G. Claros, P. Vincens, Computational method to predict mitochondrially imported proteins and their targeting sequences, Eur. J. Biochem. 241 (1996) 779–786.
[30] S. Bolte, F.P. Cordelières, A guided tour into subcellular colocalization analysis in light microscopy, J. Microsc. 224 (2006) 213–232, http://dx.doi.org/10.1111/j.1365-2818.2006.01706.x.
[31] G. Carrara, N. Saraiva, C. Gubser, B.F. Johnson, G.L. Smith, Six-transmembrane topology for Golgi anti-apoptotic protein (GAAP) and Bax inhibitor 1 (BI-1) provides model for the transmembrane Bax inhibitor-containing motif (TMBIM) family, J. Biol. Chem. 287 (2012) 15896–15905, http://dx.doi.org/10.1074/jbc.M111.336149.
[32] T.A. Reimer, I. Anagnostopoulos, B. Erdmann, I. Lehmann, H. Stein, P. Daniel, et al., Reevaluation of the 22-1-1 antibody and its putative antigen, EBAG9/RCAS1, as a tumor marker, BMC Cancer 5 (2005) 47, http://dx.doi.org/10.1186/1471-2407-5-47.
[33] S. Lang, J. Benedix, S.V. Fedeles, S. Schorr, C. Schirra, N. Schäuble, et al., Different effects of Sec61α, Sec62 and Sec63 depletion on transport of polypeptides into the endoplasmic reticulum of mammalian cells, J. Cell Sci. 125 (2012) 1958–1969, http://dx.doi.org/10.1242/jcs.096727.
[34] B. Kadenbach, M. Hüttemann, S. Arnold, I. Lee, E. Bender, Mitochondrial energy metabolism is regulated via nuclear-coded subunits of cytochrome *c* oxidase, Free Radic. Biol. Med. 29 (2000) 211–221.
[35] J.A. Nielsen, M.A. Chambers, E. Romm, L.Y.-H. Lee, J.A. Berndt, L.D. Hudson, Mouse transmembrane BAX inhibitor motif 3 (Tmbim3) encodes a 38 kDa transmembrane protein expressed in the central nervous system, Mol. Cell. Biochem. 357 (2011) 73–81, http://dx.doi.org/10.1007/s11010-011-0877-3.
[36] L. Walter, B. Dirks, E. Rothermel, M. Heyens, C. Szpirer, G. Levan, et al., A novel, conserved gene of the rat that is developmentally regulated in the testis, Mamm. Genome 5 (1994) 216–221.

[37] L. Walter, P. Marynen, J. Szpirer, G. Levan, E. Günther, Identification of a novel conserved human gene, TEGT, Genomics 28 (1995) 301–304, http://dx.doi.org/10.1006/geno.1995.1145.
[38] N. Henke, D.A. Lisak, L. Schneider, J. Habicht, M. Pergande, A. Methner, The ancient cell death suppressor BAX inhibitor-1, Cell Calcium 50 (2011) 251–260, http://dx.doi.org/10.1016/j.ceca.2011.05.005.
[39] N. Saraiva, D.L. Prole, G. Carrara, C. Maluquer de Motes, B.F. Johnson, B. Byrne, et al., Human and viral Golgi anti-apoptotic proteins (GAAPs) oligomerize via different mechanisms and monomeric GAAP inhibits apoptosis and modulates calcium, J. Biol. Chem. 288 (2013) 13057–13067, http://dx.doi.org/10.1074/jbc.M112.414367.
[40] S. Kiviluoto, L. Schneider, T. Luyten, T. Vervliet, L. Missiaen, H. De Smedt, et al., Bax inhibitor-1 is a novel IP_3 receptor-interacting and -sensitizing protein, Cell Death Dis. 3 (2012) e367, http://dx.doi.org/10.1038/cddis.2012.103.
[41] N. Demaurex, C.W. Distelhorst, Cell biology. Apoptosis–the calcium connection, Science 300 (2003) 65–67, http://dx.doi.org/10.1126/science.1083628.
[42] J.-P. Decuypere, G. Monaco, G. Bultynck, L. Missiaen, H. De Smedt, J.B. Parys, The IP(3) receptor-mitochondria connection in apoptosis and autophagy, Biochim. Biophys. Acta 1813 (2011) 1003–1013, http://dx.doi.org/10.1016/j.bbamcr.2010.11.023.
[43] S. Marchi, S. Patergnani, P. Pinton, The endoplasmic reticulum-mitochondria connection: one touch, multiple functions, Biochim. Biophys. Acta 1837 (2014) 461–469, http://dx.doi.org/10.1016/j.bbabio.2013.10.015.
[44] M.K.E. Schäfer, A. Pfeiffer, M. Jaeckel, A. Pouya, A.M. Dolga, A. Methner, Regulators of mitochondrial Ca(2+) homeostasis in cerebral ischemia, Cell Tissue Res. (2014) http://dx.doi.org/10.1007/s00441-014-1807-y.
[45] D. Rojas-Rivera, C. Hetz, TMBIM protein family: ancestral regulators of cell death, Oncogene (2014)http://dx.doi.org/10.1038/onc.2014.6.